

High-energy femtosecond stretched-pulse fiber laser with a nonlinear optical loop mirror

F. Ö. Ilday and F. W. Wise

Department of Applied Physics, Cornell University, Ithaca, New York 14853

T. Sosnowski

Clark-MXR, Inc., Dexter, Michigan 48130

Received May 29, 2002

A stretched-pulse fiber laser with a nonlinear optical loop mirror (NOLM) that produces 100-fs pulses with 1-nJ energy is demonstrated. These results constitute a 30-fold increase in pulse energy over previously reported femtosecond fiber lasers with a NOLM. Compared with previous stretched-pulse lasers, this laser offers a cleaner spectrum and improved stability, with comparable pulse duration and energy. Implications for the construction of truly environmentally stable lasers are discussed. © 2002 Optical Society of America
OCIS codes: 320.7090, 140.3510.

Fiber lasers are an attractive alternative to solid-state lasers for generation of femtosecond pulses at near-infrared wavelengths. The greater stability and compact size of fiber lasers offer the possibility of widespread application. The primary limitations of fiber lasers are insufficient environmental stability for use outside basic research laboratories and lack of high pulse energies directly from an oscillator. Environmental instability arises from uncontrolled birefringence, and the pulse energy is limited to a few nanojoules by accumulation of excessive nonlinear phase shifts. The best performance in fiber lasers is currently provided by stretched-pulse lasers^{1,2} with nonlinear polarization evolution for amplitude modulation (NPE-SPLs): 100-fs-long, 1-nJ pulses are routinely achievable. The buildup of pulses from noise and subsequent stabilization requires the use of a fast saturable absorber (SA), such as nonlinear polarization evolution³ (NPE) or a nonlinear optical loop mirror⁴ (NOLM; or, similarly, a nonlinear amplifying loop mirror).⁵ The stretched-pulse laser reduces the effective nonlinearity of the system by stretching and compressing the pulses within the cavity. This approach has led to an ~30-fold increase in pulse energy over soliton fiber lasers.

For maximum environmental stability, fiber lasers can be constructed from polarization-maintaining (PM) fiber. However, this approach precludes the use of NPE, which is based on elliptical polarization rotation. NOLM is capable of fast and deep modulation in a simple scheme and can be constructed from PM fiber. In fiber lasers, the pulse energy is limited by excessive nonlinearity through two mechanisms: soliton dynamics and overdriving of the NPE. We recently proposed the use of nonlinearity management to address the former issue.⁶ The latter mechanism arises from the interferometric nature of NPE. A NOLM operates with nonlinear phase shift accumulated only in the nonlinear loop, whereas the entire laser cavity contributes in the case of NPE. Therefore, overdriving NOLM can be prevented simply through the use of a shorter nonlinear loop.

In this Letter we consider the use of a NOLM to stabilize a stretched-pulse laser. We evaluate the performance of this laser in comparison with a NPE-SPL in our laboratory. The stretched-pulse technique is implemented to suppress spectral sidebands⁷ and for increased pulse energy. We obtain pulse energy 30 times higher than that of previously reported soliton fiber lasers with a nonlinear amplifying loop mirror.^{8,9} We arrange the total cavity dispersion to be small and anomalous while maintaining the same dispersion contrast as in a NPE-SPL. In this way, instabilities as a result of spectral sideband formation are avoided, but a much cleaner spectrum is obtained at the expense of a small decrease in pulse energy. An environmentally stable version of the laser described here can be constructed from PM fiber.

Numerical simulations of the stretched-pulse laser with a nonlinear optical loop mirror (NOLM-SPL) were used to guide the design of the laser. As a first step, operation of a NOLM itself with the appropriate pulse energy, chirp, and fiber lengths was verified numerically and experimentally. The oscillator as modeled is composed of four fiber sections. Er-doped fiber is followed by a section of standard single-mode fiber (Corning SMF28). The pulses are then split asymmetrically, traverse a dispersion-shifted fiber (DSF) in the NOLM in opposite directions, and are combined at the coupler to propagate through a final section of SMF28. Propagation within each fiber is modeled with an extended nonlinear Schrödinger equation that includes the effects of group-velocity dispersion, Kerr nonlinearity with a Raman contribution, and gain in the Er-doped fiber. The gain saturates with total energy and has a parabolic frequency dependence with a bandwidth of 40 nm. These simulations exhibit stable pulse formation over a reasonable range of parameters. Implementation of the dispersion map, Kerr nonlinearity, saturating gain, and NOLM action reproduces the basic features of the experimental observations described below. However, with the highest powers and shortest pulses, redshift of the pulses as a result of Raman scattering becomes significant. Thus,

consideration of the finite gain bandwidth is crucial. More-detailed modeling that includes a semiconductor SA and higher-order effects (such as third-order dispersion, self-steepening, and splice losses) does not influence the qualitative results.

Based on the simulations, we constructed the laser depicted in Fig. 1. The Er-doped fiber, which has a normal group-velocity dispersion of $75 \text{ ps}^2/\text{km}$, is 93 cm long. It is pumped by a 980-nm diode with total power of approximately 250 mW. The rest of the linear loop is composed of SMF28 and a small amount of Corning Flexcor 1060. The total length of single-mode fiber is 2.6 m ($\beta_2 = -23 \text{ ps}^2/\text{km}$), and the Flexcor fiber is 0.5 m ($\beta_2 = -7 \text{ ps}^2/\text{km}$). The nonlinear loop is made from 3 m of DSF ($\beta_2 \sim -3.5 \text{ ps}^2/\text{km}$). The total dispersion of the cavity is calculated to be $\sim -0.002 \text{ ps}^2$. The repetition rate is 23 MHz. A polarization-insensitive isolator provides unidirectional operation in the linear loop. Pulses are extracted from the cavity with a 30% output coupler. Placing the coupler between the NOLM and the isolator in the linear loop allows us to monitor the portion of the pulse that is rejected by the NOLM. The rejected pulse has lower quality, typically with a double-peaked spectral shape and substantial Raman shift in comparison with the output port. A variable-ratio coupler is used in the NOLM, which permits fine adjustment of the peak switching intensity. A polarization controller (PC) in the NOLM sets the linear bias. An InGaAs SA with a measured response time of $\sim 100 \text{ ps}$ and a modulation depth of 1.9% is placed between the NOLM and the gain fiber to assist initial pulse formation. Without the SA, similar pulsed operation is achieved, but stability is decreased and an external perturbation is necessary to initiate mode locking. Operation with the SA alone, without the NOLM, results in pulses in the picosecond regime.

We obtain mode-locked operation by adjusting the variable coupler (close to 50:50) for a given intracavity energy and setting the linear phase bias with the PC. Initiation of pulsing and steady-state operation corresponds to the same PC setting and pump power. Long-term stability of the laser is excellent, similar to that of the NPE-SPL: Mode-locked operation was uninterrupted over several days of continuous operation. The laser is significantly more stable against environmental effects (mechanical perturbations and temperature variations) than the NPE-SPL. The increased stability is presumably due to the fact that NOLM operation does not depend on polarization directly but is affected indirectly as changes in birefringence of the fiber shift the linear bias. Positively chirped pulses are extracted and are dechirped in 0.8 m of the fiber coupler.

The benefits of operating at small and anomalous dispersion can be seen by comparison with the NPE-SPL. Interferometric autocorrelations and the spectra of the pulses from the two lasers are compared in Fig. 2. The NOLM-SPL produces pulses with a clean, smooth spectrum much narrower than that of the NPE-SPL. Despite the significantly smaller bandwidth, pulses from the NOLM-SPL are only

slightly longer [125-fs, assuming a $\text{sech}(t)$ pulse shape considering the spectral shape] than those of the NPE-SPL (100-fs, assuming a Gaussian pulse shape). The undesirable secondary structure in the autocorrelation trace is noticeably smaller for the NOLM-SPL. The maximum single-pulse energies are comparable, 1.0 nJ for the NOLM-SPL and 1.3 nJ for the NPE-SPL. Long-range (130-ps) autocorrelations were measured to confirm the correct contrast ratio. In addition, the pulse train was monitored in the time domain with a resolution of $\sim 1 \text{ ns}$. No evidence of multiple pulsing or a pedestal was found. Comparison of second-harmonic light generated by the two lasers in a frequency-doubling crystal, as well as the autocorrelation signals, provides direct verifications of the pulse energy of the NOLM-SPL.

Fiber lasers that produce long (0.1–1-ns) noiselike pulses with broad spectra and autocorrelation signals with a narrow (femtosecond) structure on top of a very broad pedestal have been reported.^{8,10} Unless careful long-range autocorrelation scans are recorded, the pedestal may not be noticeable. Long-cavity fiber lasers with negligible or no dispersion management tend to operate in this manner when the pulse energy substantially exceeds the fundamental soliton energy. There are recent reports of nanojoule pulse energies from long-cavity fiber lasers,^{11,12} which are very difficult to understand. Based on numerical simulations and observations of long-cavity lasers in

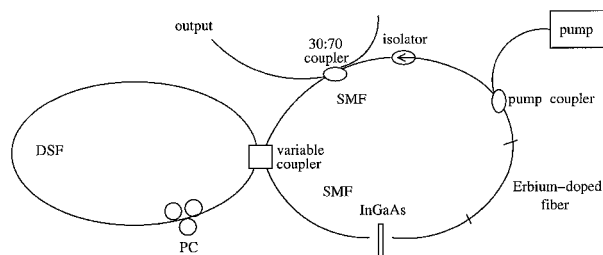


Fig. 1. Experimental setup of the stretched-pulsed fiber laser with a NOLM. DSF, dispersion-shifted fiber; SMFs, single-mode fibers.

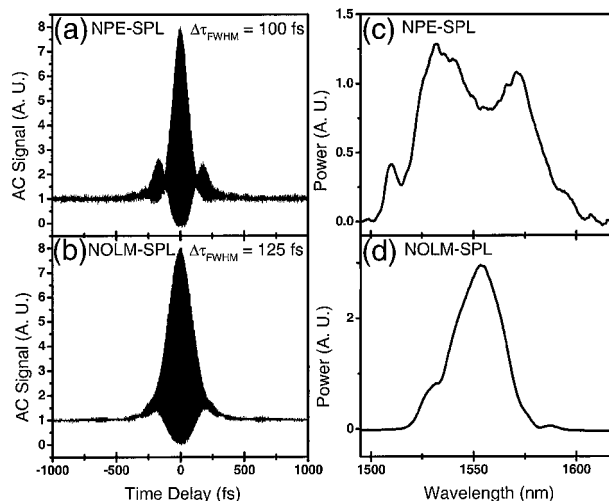


Fig. 2. Comparison of the two lasers: autocorrelation (AC) trace of (a) the NPE-SPL and (b) the NOLM-SPL and spectra of (c) the NPE-SPL and (d) the NOLM-SPL.

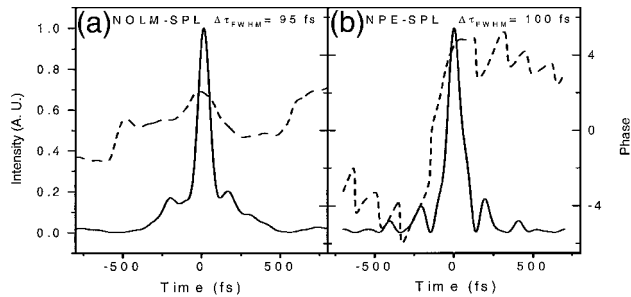


Fig. 3. Intensity (solid curves) and phase (dashed curves) profiles of the two lasers calculated with a retrieval algorithm: (a) NOLM-SPL and (b) NPE-SPL.

our laboratory, we conclude that these lasers produced noiselike pulses.

We used a pulse-retrieval algorithm¹³ to reconstruct the pulse's electric field by fitting the measured interferometric autocorrelations with autocorrelations calculated from the measured spectra and a varying phase profile (Fig. 3). The pulse profiles have approximately the same FWHM, 95 fs for the NOLM-SPL and 100 fs for the NPE-SPL. The NOLM-SPL, with its flatter phase profile, utilizes the available bandwidth more efficiently. The time-bandwidth product for the NOLM-SPL is 0.32 (0.41) if we assume 95 (125 fs) for the pulse width, compared with 0.75 for the NPE-SPL. The benefits of weaker dispersion management are not specific to the NOLM-SPL; a NPE-SPL can be built with slightly anomalous group-velocity dispersion. However, with a similar dispersion map, the NPE-SPL produces significantly lower single-pulse energies.

It is important to understand what limits the pulse energy in a fiber laser. With the anticipation that overdriving the NPE is the immediate limitation to a NPE-SPL, we built a NPE-SPL with additional output ports for characterization. These experiments reveal that a large fraction of the pulse (typically more than 70% and as high as 97%) is coupled out of the cavity at the NPE rejection port directly after the gain fiber when the laser operates with high pulse energies. Thus, only a small fraction of the pulse energy (<0.5 nJ) circulates in the cavity on the average, which greatly reduces the effective nonlinearity. The corresponding pulse energy of the NOLM-SPL reported here is close to 2 nJ after the output coupler. After accounting for internal losses, we estimate the average pulse energy inside the NOLM-SPL to be approximately three times higher than in the NPE-SPL. This strongly suggests that overdriving the NPE is indeed the first limitation to the pulse energy for the NPE-SPL. Further increases of the energy of the NOLM-SPL produce multiple pulsing. When the length of DSF in the NOLM is decreased, mode locking becomes difficult. Therefore, experimental results are inconclusive as to whether the NOLM-SPL described here is currently limited by

overdriving NOLM or the nonlinearity is simply too high for a single dispersion-managed soliton under these conditions. Numerical simulations that isolate the effect of the NOLM suggest that it is the latter. We conclude that a strongly stretched-pulsed laser is a route to obtaining higher pulse energies than has been possible to date, provided that overdriving the SA is avoided.

In conclusion, we have demonstrated a stretched-pulse laser stabilized by a NOLM that produces 1-nJ and 100-fs pulses. These are to our knowledge the highest femtosecond pulse energies obtained by a fiber laser with a NOLM. Implementation of mild dispersion management produces a clean spectrum and close to transform-limited pulses. Although this constitutes a small trade-off in pulse energy, a clean spectrum is highly desirable for applications such as amplification, frequency doubling of the pulses, and spectroscopic measurements. Higher intracavity pulse energy has been obtained with the NOLM-SPL than with the NPE-SPL, indicating that overdriving the SA (i.e., the NOLM or NPE) is the immediate limitation to higher energies. By demonstrating performance comparable to or slightly exceeding that of the NPE-SPL, we identify a route to an environmentally stable, all-PM fiber laser that produces high-energy, femtosecond pulses in a simple scheme.

This work was supported by the National Institutes of Health under grant RR10075. The authors thank Matthew Bolcar for help with numerical simulations. F. Ö. Ilday's e-mail address is foil@cornell.edu.

References

1. M. Hofer, M. H. Ober, and M. E. Fermann, *IEEE J. Quantum Electron.* **28**, 720 (1992).
2. K. Tamura, E. P. Ippen, H. A. Haus, and L. E. Nelson, *Opt. Lett.* **18**, 1080 (1993).
3. M. Hofer, M. E. Fermann, F. Haberl, M. H. Ober, and A. J. Schmidt, *Opt. Lett.* **16**, 502 (1991).
4. N. J. Doran and D. Wood, *Opt. Lett.* **13**, 56 (1988).
5. M. E. Fermann, F. Haberl, M. Hofer, and H. Hochreiter, *Opt. Lett.* **15**, 752 (1990).
6. F. Ö. Ilday and F. W. Wise, *J. Opt. Soc. Am. B* **19**, 470 (2002).
7. S. M. J. Kelly, *Electron. Lett.* **28**, 806 (1992).
8. D. J. Richardson, R. I. Laming, D. N. Payne, M. W. Phillips, and V. J. Matsas, *Electron. Lett.* **27**, 730 (1991).
9. M. Nakazawa, E. Yoshida, and Y. Kimura, *Appl. Phys. Lett.* **59**, 2073 (1991).
10. M. Horowitz, Y. Barad, and Y. Silberberg, *Opt. Lett.* **22**, 799 (1997).
11. For example, see T. O. Tsun, M. K. Islam, and P. L. Chu, *Opt. Commun.* **141**, 65 (1997).
12. See also E. A. Kuzin, B. Ibarra Escamilla, D. E. Garcia-Gomez, and J. W. Haus, *Opt. Lett.* **26**, 1559 (2001).
13. J. W. Nicholson, J. Jasapara, W. Rudolph, F. G. Omenetto, and A. J. Taylor, *Opt. Lett.* **24**, 1774 (1999).